Dalton Transactions

Accepted Manuscript

ROYAL SOCIETY OF CHEMISTRY

www.rsc.org/dalton

Original paper submitted for publication in
Dalton Transactions

The chemical drop of elastic properties in zeolites: comparison of formation of carbonate species *versus* dealumination

Bryukhanov I.A.[a], Rybakov A.A.[b], Kovalev V.L.[a], Larin A.V.[b*], Zhidomirov G.M.[b, c]

[a]*Department of Mechanics and Mathematics, Moscow State University, Leninskie Gory, Moscow, GSP-2, 119992 Russia,* [b] *Chemistry Department, Moscow State University, Leninskie Gory, Moscow, GSP-2, 119992 Russia,*
[c] *Boreskov Institute of Catalysis, SO RAN, Novosibirsk, 630090, Russia*

*) *corresponding author:* nasgo@yandex.ru

Other e-mail addresses are

Bryukhanov I.A. *ibryukhanov@gmail.com*

Rybakov A.A. *rybakovy@gmail.com*

Kovalev V.L. *valerykovalev@yandex.ru*

Zhidomirov G.M. *zhidomirov@mail.ru*

TOTAL PAGES 25

TABLES 2

FIGURES 5

SUPPLEMENTARY ELECTRONIC MATERIALS – YES

Abstract

The decrease of elastic moduli (Young's, bulk, and shear modulus), the variations of their asymmetries, of the Poisson's ratio and of the linear compressibility due to the carbonate formation in NaX has been compared to that produced by dealumination of HY framework (from Al-Si-Al fragment positioned in joined 4R rings). All the systems have been considered at the DFT level using periodic boundary conditions. The representativeness of the models has been checked *via* comparison of calculated IR spectra of carbonate and hydrocarbonate species in NaX and of hydroxyl groups in HY to the experimental ones. The correlation between the destabilization energy of the systems and the displacements of Na or K cations coordinated to the carbonate or hydrocarbonate species, *i.e.,* expressed *via* Me-O bond elongations, has been observed for both one or two carbonate and hydrocarbonate species per unit cell. Finally, the similar loss of the elasticity by the FAU zeolites has been obtained due to either carbonate / hydrocarbonate formation in NaX or a step of HY dealumination.

Keywords: elastic modulus, DFT, carbonate, dealumination, FAU, alkali cation

1. Introduction

The preparation of zeolites and sieves for selected industrial process is a complex multi-step procedure whose separate stages (deleting of templates, dehydroxylation, thermodesorption, *etc.*) can induce different internal strains being important for a final mechanical stability of the catalyst. The effect of weakening of elastic properties in the course of chemical reaction is an old topic which had been more extensively discussed for external surfaces of solids or alloys [1, 2]. Theoretical classification of such defects as well as of the results of the reactions with diffusing

gases in zeolite or metal-organic framework (MOF) pores and a quantitative measure of their at least relative influences can seriously help to rationalize the production of resistant and stable catalytic materials. However, it is difficult to link the atomic level parameters with the macroscopic parameters characterizing the elasticity. In many cases the possibilities to consider such a solution at the quantum chemistry level are blocked by the large size and aperiodic character of defective domains. However, some zeolites with a unit cell (UC) of moderate size permit such analysis at the microscopic level. Due to the possibility of reagent penetration throughout the pores the reaction passes in nearly continuous way in the zeolites or the MOFs changing the elastic moduli (EM). Then the reactive system can be treated using periodic boundary conditions (PBC). Hence, the EM calculation *via* stiffness matrix can be performed with nowadays computational facilities using DFT methods with plain wave [3] or crystalline orbitals (CO) as linear combinations of atomic orbitals (LCAO) [4] basis sets with VASP [5] and CRYSTAL [6] codes, respectively. These opportunities have led to immediate growth of interest to the correlations between the hardness of porous crystals and their structures [7-9]. Additionally, a software for the respective analysis has been recently developed [10, 11] which has facilitated and expanded the range of elastic modulus to interpret. As a result, new features of the zeolites and MOFs have been recently discussed, *i.e*., the negative linear compressibility for some forms of all siliceous zeolites [9] similarly to those in MOFs and the smallest eigenvalue of the positive definite stiffness matrix as new criterion to be related with the structure compliance [8].

A relevance of physical effects (capillary condensation [12, 13], Xe [14, 15] or CO_2 [16-18] adsorption) to modify the elastic properties of the zeolites [14, 16-18] or MOF [16] has been shown. But analogous chemical influence has not yet been described numerically with one exclusion. Earlier, we have demonstrated that the carbonate formation can worsen the elastic properties (Young's, bulk, and shear modulus) of the NaX and NaKX zeolites using PBC and

molecular mechanics with different core-shell force fields (FFs) [19]. This approach had been enough to reveal the main effect of the competition between two different types of anions, *i.e*., between framework lattice and carbonates, which try to coordinate alkali cations. Surely, such an effect needs to be confirmed at a higher computational / theoretical level. We have undertaken such an attempt to check the same behavior of the EM of the NaX and NaKX zeolites at the DFT/(LDA [20], PBE [21]) level with PBC. To realize the general comparison of the zeolite defects of different types as formulated in the beginning and to compare the measure of the EM weakening due to carbonate formation we have performed similar EM calculations upon the dealumination of HY framework. The extraction of one Al atom may be considered as a step to prepare, for example, the USY forms. This stage looks like a direct damage of the FAU framework which should definitely worsen its elastic properties. Hence such a comparison makes the loss of elasticity due to the carbonate activity more "measurable" and understandable value. As an intermediate step of the HY dealumination we have stopped it at the formation of the hydrated $AlOH^{+2}$ species whose presence in the products of the dealumination has been confirmed with NMR techniques [22-24].

In the next parts the computational details (part 2), the geometry of the optimized X zeolites (part 3.1.1), the changes in their elastic properties (part 3.1.2), and total energy (part 3.1.3) are presented and compared to similar effect of HY dealumination regarding EM values (part 3.2).

2. Computational details

We have optimized the fractional coordinates and cell parameters of the MeX zeolites with and without the CO_3^{2-} and/or HCO_3^- species, Me = Na and K, using both the local density approximation (LDA) in the Ceperley-Alder version (CA) [20] and the generalized gradient

approximation (GGA) PBE functional [21] as implemented in the VASP package [5]. In the $Na_4K_{20}Si_{24}Al_{24}O_{96}\times nH_2CO_3$ (NaKX), n = 0 – 2, only K cations are attainable for the contacts with carbonates, Na being in the SI site (inside the D6R prisms). The NaX formula thus corresponds to $Na_{24}Si_{24}Al_{24}O_{96}\times nH_2CO_3$. The carbonate formation has been modeled *via* the reaction from H_2O and CO_2. All trial geometries have been constructed with CO_3^{-2} species in NaX with the exception of some cases in NaKX where HCO_3^- species or CO_3^{2-}/HCO_3^- pairs have been also tested as initial geometries.

The projector augmented wave (PAW) method [25] has been applied to describe electron–ion interactions, and a plane wave basis set has been employed for the valence electrons. An appropriate plane-wave cutoff of 500 eV was set for the pseudopotentials. The most of the results have been calculated in the Γ–point. Comparative calculations in the Γ–point and using the 3×3×3 *k*-grid showed the difference of 0.05 eV in the energy and 1.0 cm^{-1} in the frequencies. The stiffness matrix has been calculated *via* finite differences as adopted in VASP [5], then respective elastic constants have been calculated using the algorithm presented in Supplementary Electronic Materials (SEM) of the ref. [8]. The elastic constants have been averaged according to the Hill scheme [26]. Graphical analyses of the asymmetry of Young *modulus* (YM) in Cartesian coordinates calculated at the DFT/LDA level in the NaX zeolite has been performed using the Mathematica code [11]. Calculated IR spectra of carbonate and hydrocarbonate species in NaX have been compared to the experimental ones [27, 28]. No scaling for calculated vibrational frequencies has been applied to match experimental ones. The DFT-D2 approach [29] has been used to evaluate the importance of the dispersive terms.

The initial $H_{12}Si_{36}Al_{12}O_{96}$ (HY) structure and three semi-products of its dealumination have been fully optimized and the respective frequencies have been calculated in the Γ–point to verify an agreement with the experimental IR spectra [30, 31]. After rupture of two Al-O bonds of the selected Al atom in HY the $H^+(H_2O)_2$ group has been added to the system nearby the Al

atom and the geometry optimization has been performed. During each of the two subsequent steps one water molecule was added to the system with the following geometry optimization.

3. Results

3.1 Carbonate formation

3.1.1 The geometry optimization

Framework geometry. The geometry optimization has led to coherent results obtained with FFs [19] and DFT for NaX predicting slight increase of UC volume (ΔV) upon the formation of one or two carbonate moieties (Fig. 1a and Table S8). Each four models (Fig. 1a) with one (left) and two (right) carbonate species per UC, respectively, are ordered from left to right from the most stable to the less stable one as in Table S8 (as similarly shown from top to bottom *via* relative energies in Table S9). For one carbonate particle the ΔV increase is larger with LDA, *i.e.*, 0.58 % for the favored site (Na151 model in Table S8) and the maximum is 0.96 % (Na149), as compared to those with Catlow FFs, *i.e.*, 0.22 % for the favored site (Na151 model in Table 1 of ref. [19]) and the maximum is 0.45 % (Na152 case therein). The agreement is better between LDA and Sauer-Sierka FF for any (1 or 2) carbonate moieties per UC of NaX. The results obtained using PBE predict the smaller ΔV changes being less than 0.3 % and which can be even minor negative for one carbonate species at favored site (-0.01 % in Figure 1). However, the agreement between the predictions of the PBE and Sauer-Sierka FF for NaKX is surprising because both approaches show a negative ΔV upon the formation of two carbonate species (Fig. 1a, Table S8). More precisely, adsorption of the two pairs (CO_2 and H_2O) of molecules leads to a contraction of UC with DFT (PBE) and molecular mechanics (Sauer-Sierka FF) despite of the additional volume of the molecules. In the case of the reaction when one pair (CO_2 and H_2O) of molecules produces one carbonate moiety the results differ. The FF approach

shows the contraction of UC while the PBE shows no changes at the favored site (Na151 in Table S8) and is positive within less than 0.25 % for all other considered cases.

Carbonate geometry. The formation of two pairs of the carbonate bands in NaX had been shown in different works as 1715 and 1365 cm^{-1} (with the difference between the high and low frequency peaks or band splitting (BS) of 350 cm^{-1}) and 1425 and 1485 cm^{-1} (BS = 60 cm^{-1}) [27, 28]. The pair at 1715 and 1365 cm^{-1} had been assigned to a carbonate in asymmetric site [27]. These works [27, 28] had not fully assigned the spectra because the peaks at 1580 cm^{-1} in NaX and 1670 cm^{-1} in KX [27] had been classified neither to carbonate, nor to CO_2. All of the BS values can be interpreted in the terms of asymmetry parameter δ or bond distortion of CO_3^{-2}:

$$\delta = \Sigma_{i=1}^{3}(||C\text{-}O|_i - |C\text{-}O|_{aver}|) \quad (1)$$

relative to the average value $|C\text{-}O|_{aver} = (\Sigma_{i=1}^{3}|C\text{-}O|_i)/3$ in the carbonate with a high accuracy [32]. The optimized carbonate geometries have been below described in the terms of the asymmetry parameter δ. The carbonates remain stable in all the models with one CO_3^{-2} species per UC of NaX with both DFT approaches with $\delta < 0.056$ Å. In some NaX models with two carbonates per UC the HCO_3^- moiety has been obtained from CO_3^{-2} owing to protons available in the cages[1] and which can be captured by CO_3^{-2}. The final geometries of both asymmetric hydrocarbonate (δ = 0.200 and 0.197 Å at the PBE level or 0.224 and 0.137 Å using LDA) and nearly symmetric carbonate (δ = 0.020-0.021 and 0.021-0.023 Å at the PBE and LDA levels, respectively) forms has been optimized by us in NaX.

The accuracies of the BS predictions basing on the BS(δ) earlier fitted [32, 33] are shown in part S1 of SEM. The most accurate matching of the experimental BS data for carbonate and hydrocarbonate is obtained for the most stable model with PBE approach (Table 1), *i.e.*, 58.6 and

[1] We remind that protons were also located in the NaX or NaKX cages while computing the same systems with FFs in ref. [19].

332.7 cm^{-1} (no scaling) *versus* experimental values of 60 and 350 cm^{-1} [27, 28]. To our best knowledge, the spectra of the carbonates and hydrocarbonates in NaX have been modeled in a reasonable agreement with the experimental ones for the first time. This coincidence for both carbonate and hydrocarbonate BS values confirms an adequacy of the NaX models. This also allows us to conclude that hydrocarbonates in NaX should be responsible for the peak with BS value of 350 cm^{-1} instead of proposed earlier asymmetric carbonate [27].

The CO_3^{-2} moieties do not trap proton in all the NaKX models irrespective of one or two carbonates per UC. The introduction of the CO_3^{-2}/HCO_3^- pair (Table S9) in the initial NaKX instead of two CO_3^{-2} species has led to a stable geometry with a reasonable large BS value (Table 1) *versus* experiment [30, 31]. One should mention their superior stabilities as compared to analogous (156, 152) model with two CO_3^{-2} species in NaKX as much as 1.57 eV at the PBE level (Table S9). Regarding the absence in NaKX of small experimental BS values which are typical for CO_3^{-2} [32] and also calculated in NaX herein (Table 1), one could propose a formation of only HCO_3^- (and not of CO_3^{-2}) in NaKX. It had been calculated in the RHO framework [33] that the reaction of the CO_3^{-2} formation is less exothermic (and is within a domain upper limited by Si/Al ratio) than that of the HCO_3^- formation. The author [33] had not succeeded to find a route for an exothermic CO_3^{-2} formation (as obtained for HCO_3^-) neither in the Na5K1RHO, nor in the Na1K5RHO forms, but both species had been modeled *via* exothermic reactions within the Na6RHO framework. The different cationic mobilities of Na and K can be one of the reasons of the heat values. The lower mobility of K cations is not confirmed herein by the tighter coordination by K cations to the carbonates in NaKX (Fig. 2c, d). For the first look this lower mobility of the K^+ cation has been illustrated in ref. [34] regarding the lowest K^+ diffusion coefficients relative to that of Na^+ (Fig. 6 of ref. [34]). But this lower mobility is in a partial contradiction with the larger amplitude of K^+ shift from the plane of the 8R window than that of Na^+ in the course of CO_2 passing through it as obtained by the *ab initio* MD simulations in the

LTA framework [35] (Fig. 7 in ref. [35]). That is why we believe that K^+ mobility is high enough owing to the smaller K^+ electrostatic interaction with the framework (as also discussed below in the part 3.1.3). The most probable reason of only HCO_3^- (and not of CO_3^{-2}) formation is the higher kinetic barrier for CO_3^{-2} formation in NaKX or KX. They had not been evaluated for NaKRHO forms in the ref. [33]. We suspect that both the formation reactions can possess the barriers of distinct heights and out first computational attempts confirm this. Our optimizations herein have shown that the HCO_3^- formation from CO_3^{-2} can pass even *via* a barrierless route in NaX in accordance with experiment if a proton is attainable closely to CO_3^{-2} [30, 31] but it is not a typical situation for other X forms which do not prompt the CO_3^{-2} formation.

Resuming this part, one should note that the carbonate and hydrocarbonate frequencies calculated in NaX using PBE suit evidently better to the experimental ones than those obtained with LDA.

3.1.2 The calculation of the elastic properties

For NaX all variety of the DFT and FF methods has been applied. The EM values are maximum decreased with LDA, while other results are similar and show the moderate changes, *i.e*., within -5.2 and -5.7 % with PBE, upon the influence of one and two carbonate moieties, respectively (Fig. 1b, Table S9). The LDA results remain an upper boundary for the EM changes in NaX including earlier calculations using molecular mechanics with any of two FFs applied in ref. [19]. Minimal and maximal values of Young's modulus (E) (Fig. 1b), shear modulus (S), Poisson's ratio (ν), respective asymmetries $A_X = X_{max}/X_{min}$, X = E, S, and linear compressibilities β_x, β_y, β_z, in the NaX and NaKX models are shown in Table S10. The case of the A_E asymmetry is illustrated graphically in Fig. S3 with the help of the Mathematica code [11]. The minimal and maximal values for the YM as well as for the shear moduli (Table S10)

decreases as much as 5-13 % with LDA, while only the upper values decrease with the carbonate formation using PBE (1-7 %). The minimal and maximal YM and shear values nearly conserves in NaKX. In accordance with the results of ref. [9], where all siliceous FAU framework of the Y type has not shown the negative linear compressibility [9], we have observed only positive terms of linear compressibility (Table S10). Only positive Poisson's ratios for all NaX and NaKX models have been obtained (Table S10). The A_X values for both X = E, S are relatively small as for the MOF-5 and ZIF-8 type MOFs [7] and manifest different behavior with LDA or PBE regarding the addition of the second carbonate species. The asymmetries for E and S increase while adding first or second carbonates for the models calculated using LDA but they either do not effectively vary (E), or drop (S) for the models calculated using PBE with some exceptions. It can signify that the weakening of the FAU structure has no an emphasized anisotropy using PBE when the change of the A_E cannot be remarked by eye after the addition of carbonate species. The PBE method seems to be more adequate for our models regarding the better coincidence of calculated frequencies with the experiment (Table 1). The minimal eigenvalue of the stiffness matrix (not shown) remains much larger (> 10 GPa) than those for the MOFs (~ 0.1 GPa) [7, 8] irrespective of the addition of one or two carbonate species at both (LDA, PBE) levels. Hence, these variations do not manifest a formation of any soft deformation mode owing to the carbonates.

The main difference between the EM obtained for NaKX within two different approaches, *i.e.*, molecular mechanics [19] and DFT, is related to the different extents of the EM variation upon the carbonate influence (Tables S3, S9). Large changes are predicted with Sauer-Sierka FF in opposite to the moderate decreases calculated using PBE/PAW. If the intervals of the EM decreases for NaX calculated with DFT and FF methods intersect, they do not in the case of NaKX (Table S9). The partial compensation of the EM drop due to the carbonates in NaKX could come from the larger K radius which strengthens the rigidity of the X framework.

Possibly, the latter can be described properly within the scope of DFT methods only as it requires a proper presentation of all energy components. The latter cannot be calculated with FF approaches[2]. The changes in the bulk and shear modulus are presented in Table S3 of SEM. They mainly repeat the trends calculated for the YM for one and two carbonate moieties with any method. To illustrate the measure of these EM falls we have compared them with the EM drops during the HY dealumination (part 3.2).

3.1.3 The relation between destabilization energy and cationic drift

The models containing two carbonate species per UC as calculated with DFT methods are more complex and diversified than those obtained using FF approach. One of two carbonates in four models (two LDA and two PBE cases, denoted by stars in Tables S9) transforms to hydrocarbonate *via* barrierless reaction. It is a consequence of the higher thermodynamic stability of hydrocarbonates earlier discussed in ref. [33][3]. Hence, if a barrier to trap proton from a framework is absent in the selected geometry then carbonate gives hydrocarbonate. The heat of the carbonate and hydrocarbonate formation was studied as a function of the Si/Al moduli in the Na_xCsRHO forms in the interval $2.43 < Si/Al < 7.0$, where x depends on the moduli varying as $2 \leq x \leq 6$, respectively [33]. The comparison with Na_xCsRHO is justified because only one Cs cation is included and Na remains a dominant cation in both systems therein [33] and herein. Respective fitted parameters of the linear $\Delta U(Si/Al)$ functions [33] allow extrapolation to the $Si/Al = 1$ for our NaX case (see part S2 of SEM). It leads to the higher (in absolute value) heat of the hydrocarbonate formation as much as 0.796 eV. This value is just between the differences of 0.810 eV or 0.463 eV (0.463 eV = 0.810 eV – 0.347 eV in Table S9) for the models with one

[2] Owing the charge transfer neglection within molecular mechanic methods the electrostatic energy value is also distorted.

[3] We remind that all trial geometries have been constructed inducing CO_3^{-2} species and protons in the NaX framework.

hydrocarbonate species formed of two considered with the same PBE/PAW approach as used in ref. [33]. The difference of 1.570 eV between of the heats of analogous (156, 152) models of NaKX with two CO_3^{-2} or CO_3^{-2}/HCO_3^- species, *i.e.*, U_2 = -1252.200 or -1253.770[b)] eV (Table S9), respectively, is even higher than 0.796 eV obtained from the data of ref. [33].

In ref. [33] the better capability of carbonates to pull the cations from their crystallographic positions in MeRHO than that of hydrocarbonates has been remarked regarding a cation deviation from the plane of 8R window. The opposite picture, *i.e.*, the better detachment of the cations from the plane of 6R window by hydrocarbonate, has been observed in the NaX case herein. Another parameter has been applied to quantify this perturbation. More precisely, the sum of the elongations of Me-O bonds between Me cations and three nearest O atoms of the 6R windows ($\Sigma_{i=1}^{3}\Delta R_{Me\text{-}Oi}$ values from Table S1 or Fig. 3a) has been considered to evaluate the capability to pull the cations. The sum is larger for the hydrocarbonate for two cases of the total four when the hydrocarbonates have been obtained in NaX ($\Sigma_{i=1}^{6}\Delta R_{Me\text{-}Oi}$ values from Table S2 or Fig. 3b, where index "*i*" in summation spans three O atoms in two 6Rs for carbonate / hydrocarbonate species). These larger displacements of one of the Na cations have not led to the worse stabilities because of the compensation from the higher heat of the hydrocarbonate formation compared to the one of carbonate moiety (Fig. 1b) mentioned above. It is instructive to compare Fig. 3 with the similar presentation of the data obtained using FFs [19] in Fig. S1 of SEM. No any correlation is found between the stabilities and the elongations of the Me-O bonds. Partly, the reasons of the difference are related with the formation of hydrocarbonates. It can be properly modeled using DFT only, while the FFs used in [19] have not been constructed in the way to involve such a possibility. However, the relations between the models (153, 149) and (155, 151) in which HCO_3^- species are formed with both LDA and PBE methods show more complex behavior with respect to $\Sigma_{i=1}^{6}\Delta R_{Me\text{-}Oi}$ values. Additional stabilization owing to hydrogen bonding (HB) is smaller for the (155, 151) model in both LDA and PBE cases than for

(153, 149). For the latter, the short HB lengths are 1.789 and 1.799 Å using LDA and PBE methods *versus* 2.460 and 2.349 Å, respectively, for the (155, 151) one. This HB length corresponds to rather strong energy gain, because comparable HB length evaluated as 1.874 Å (X-ray data [36]) or 1.758 Å (periodic Hartree-Fock calculations [37]) between two water molecule is the reason of extremely stable $AlPO_4$-15 sieve (or ADP) structure containing this pair. Thermo-desorption of the first water molecule leads to a partial ADP collapse [38]. But only in one (153, 149) case the additional HB contribution to the total energy leads to favored stability of this model. It signifies that the HB energy term can explain only the slight deviation of the point with the coordinates ($\Sigma_{i=1}^{6}\Delta R_{Me\text{-}Oi}$, ΔU) = (0.439, 0.347) with PBE (Fig. 3b), but not the strong deviation of the (153, 149) model at the point with the coordinates ($\Sigma_{i=1}^{6}\Delta R_{Me\text{-}Oi}$, ΔU) = (0.139, 0.305) with LDA. In the absence of HCO_3^- species in NaKX the monotonic ΔU increase has been obtained with the cation displacements (shown by diamonds in Fig. 3b). The simple evaluations have been performed to show a negligible influence of the repulsive Coulomb energy between two carbonate species (see part S3 and Table S4 of SEM) which cannot thus be the reason of this fluctuation using LDA.

The larger amplitude of the K drift (Fig. 1, Tables S1, S2) leads to the lower destabilization energy (Table S9) than the one due to the Na drift[4]. The electrostatic nature of this behavior can be proposed. Despite the closeness of the calculated Bader type charges of Na and K which are 0.872-0.908 and 0.847-0.904 *e* in the NaX and NaKX (Table S7), the difference in the ionic radius, *i.e.*, 0.99 and 1.37 Å [39], respectively, can be the reason of essentially different carbonate interactions with the cations. Because the radius is induced directly as a parameter in a FF method, this variation in the Coulomb energy can be evaluated using molecular mechanics. For example, the essential difference between the Na or Rb radius upon

[4] One should note that we had not observed a relation between the destabilization energy and the MeII…O_z elongations using the FFs in the ref. [19] (see part S2 and Table S5 of SEM of this ref.). The data of Table S5 from ref. [19] are shown in Fig. S1 (see SEM for the current work).

the similar charges (fitted as 0.8 and 0.75 e, respectively, in Ref. [40]) was already discussed to be the reason of distinct CO location in NaY or NaRbY (see, for example, Figure 3 in Ref. [40]) and of the different roles of closest Na or Rb cations in the total electrostatic field at the CO position nearby (see, for example, field variation in Table 5 in Ref. [40]).

Surprisingly, this variation of destabilization energy from Na- to K-forms is rather slight at the level of molecular mechanics using Sauer-Sierka FF, *i.e.*, from 0.049-0.594 to 0.117-0.432 eV for one carbonate species and from 0.695-1.130 to 0.281-0.880 eV for two carbonate species, respectively [19][5]. For comparison, the PBE/PAW leads to the drops from 0.115-1.042 to 0.016-0.331 eV and from 0.347-1.072 to 0.409-0.540 eV for one and two carbonate species, respectively (Table S9)[6]. However, the main factor which might explain the larger drop in the Coulomb energy calculation with DFT than using FF methods seems to be the fixed atomic charges in the last case. Molecular mechanics usually neglects the variation of the atomic charge due to a charge transfer (CT). In our case the carbonate charge could vary owing to the carbonate coordination with different (Na, K) cations. The Bader partition scheme for the electron density at the PBE/PAW level is available with VASP [5]. For a first glance, it overestimates[7] the charges (Tables S5, S7) thus hindering to illustrate the minor CT differences. More precisely, the carbonate charges in NaX (-1.883 and -1.918 *e* in Table S5) are comparable to that in NaKX (-1.908 and -1.904 *e*). Nevertheless, a relevant series of the neutral and charged cluster models (Fig. S2) with the appeal to the Mulliken type charges also shows that the CT varies very slightly between the Na- and K-clusters, *i.e.*, in carbonate charges are -1.272 and -1.258 *e* with the difference 0.014 e of the same order of value or even smaller as estimated in the Bader scheme above (Table S6). Hence, the agreement between small CT variation with last two examples and Bader or Mulliken type charges have shown another possible cause of the different destabilization due to either Na, or K cations. It allows to think that bulky K cations provide the

[5] Three less stable models from Table 3 of the ref. [11] determine the boundaries of the energy interval.
[6] Three less stable models from Table 2 at the PBE/PAW level determine the boundaries of the energy interval.
[7] Even the HCO_3^- charges (-1.466 and -1.385 *e* in Table S5) are essentially higher (in absolute value) than -1 *e*.

better coordination and a "neutralization" of the carbonate charge than Na ones thus lowering the repulsive Coulomb energy between the oxygen atoms of the zeolite and the carbonate. The denser coordination of the K cations in NaKX (Fig. 2c, d) than that of Na ones in NaX (Fig. 2a, b) does not contradict to this proposition. The drastic difference with the "neutralization" of the carbonate using FF schemes can be evaluated from Fig. 1b of the ref. [19] (the Figure is also used as Graphical Abstract being available on-line). There are four K cations around the CO_3^{-2} species but the K…Oc distances span the interval from 2.915 to 3.239 Å [19] to be compared with 2.577-2.905 Å or 2.645-2.988 Å with PBE/PAW herein (Table S7). Hence, the last PBE/PAW approach provides a better shielding effect for the CO_3^{-2} species by K cations than with the FF method. Finally, such an interpretation is in line with the main reason of the destabilization due to the repulsion between the framework and the obtained carbonates. Then the correlation between the destabilization energy and the cation drifts (Fig. 3) has to play a secondary role. More details are discussed in the part S4 of the SEM.

3.2 The Young's moduli variation in the dealumination process

The changes in the elastic properties (part 3.1.2, Table S9) due to a carbonate formation are rather new to a reader and are to be compared within more conventional scale of analogous variations which are better known to the zeolite community. We have considered the case of the extraction of one Al atom from joined 4R rings of the HY framework in the course of its dealumination. Such a replacement can be not complete, *i.e.*, without the following partial replacement by Si atoms, so that extra framework Al (EFAL) species like hydrated $Al(OH)^{+2}$ (Fig. 4b-d) remains inside being linked to the initial position of the Al atom and thus blocking the assessment of Si-containing compounds to this site. These results will be shortly given herein

for a comparison with the EM decrease due to the carbonate formation and will be discussed in more detail elsewhere.

This way of the dealumination from joined 4R rings containing Al-Si-Al fragments had been proposed as the most probable one in many works [41-42 and the refs. therein]. The HY has been fully optimized (Fig. 4a) and characterized with calculated IR peaks (Fig. 5). The bands at the 3659-3636 cm^{-1} (the series of the H-O1 groups in 12R windows) and 3537 cm^{-1} are in good agreement with 3642 and 3545 cm^{-1} [28] or 3643 and 3540 cm^{-1} (Fig. 5) [27]. We have not studied the fully Al/Si replaced product interesting in the effect of the HY weakening after Al extraction. At the first step the HY(D) (Fig. 4b) has been obtained after a rupture of two Al-O bonds of the selected Al atom and the attack of $H^+(H_2O)_2$ group (Fig. 4a). After this step the EFAL atom is present in the $AlOH^{+2}(H_2O)$ form which becomes $AlOH^{+2}(H_2O)_2$ at the next steps of H_2O addition and optimization (Figs. 4c, d for N = 3, 4 in Table 2). The stabilization of the dealuminated HY framework with water compensates the energy losses of the first reaction step so that the energy difference of 1.055 eV after addition of all four water molecules becomes close to that of NaX containing one carbonate species (1.042 eV for the Na150 in Table S9). The inclusion of third H_2O molecule switches the Al coordination because it losses the bond with framework oxygen while forming new bond with water oxygen. It is also accompanied by a slight compensation of the YM drop from -9.9 % to -7.2 % (Table 2) but the origin of this YM variation is evidently a discussable topic. Our guess about the relation between the change of the EFAL coordination and the YM compensation is partly confirmed by the conservation of the EFAL coordination upon the addition of fourth H_2O molecule when the change of the YM value is minor (-7.0 instead of -7.2 % in Table 2). The leaching effect of water is also confirmed by the decreasing (in absolute value) ΔV variations as -0.24, 2.6×10^{-3}, and -1.5×10^{-2} % upon the addition of two, three, and four molecules per UC, respectively (Table 2).

Minimal and maximal values of Young's modulus (E), shear modulus (S), Poisson's ratio (ν), and respective asymmetries $A_X = X_{max}/X_{min}$, X = E, S, in the four HY(D) models are shown in Table S10. The FAU framework of the Y type has also shown relatively small asymmetry (as compared to the MOF types for examples in ref. [7, 8]) similarly to NaX or NaKX. The A_E and A_S values behave differently, showing minor variations (A_E) or increasing (A_S) in the course of the addition of water molecules. Both minimal and maximal YM or shear moduli (Table S10) decrease with addition of water using PBE in opposite to the addition of the carbonates at the same computational level. The set of obtained parameters is too short to make any valuable conclusion about the trends.

4. Conclusions

DFT calculations of elastic properties (YM, bulk, shear modulus, their asymmetries, Poisson's ratio, and linear compressibility) have been performed using periodic boundary conditions for the two groups of systems where chemical reactions take place and lead to a reconstruction. The impact on the elasticity and total energy of the carbonate and hydrocarbonate formation in $Na_{24}Si_{24}Al_{24}O_{96}$ (NaX) and $Na_4K_{20}Si_{24}Al_{24}O_{96}$ (NaKX) zeolites, on one hand, and of dealumination of $H_{12}Si_{36}Al_{12}O_{96}$ (HY) framework, on the other hand, has been studied. The changes in the elastic properties owing to the formation of the carbonate species with the cations in NaX and NaKX have been also compared to those calculated earlier using molecular mechanics with two different force fields. The valuable difference between the destabilizations at the DFT and FF levels has been observed with respect to the NaKX case. The weaker influence of the carbonates at the DFT level has been assigned to the better shielding effect of the CO_3^{-2} species by K cations than with the FF method. It results in the weaker Coulomb repulsion between the oxygen atoms of the zeolite and the carbonates. The correlation between

destabilization energy of the systems and the displacements of Na or K cations coordinated to the carbonate and hydrocarbonate species has been observed using the DFT schemes for one or two carbonate and/or hydrocarbonate species per unit cell (UC). The latter is absent within the scope of the FF schemes. The measure of the cation displacements has been expressed *via* Me-O bond elongations from O atoms of the 6R at the SII sites. The lower impact of the hydrocarbonate species on the destabilization than the one of the carbonates has been obtained while comparable shifts of the Na and K cations from their O sites in the 6R windows are induced by carbonate or hydrocarbonate species.

The similar effects on the elasticity of two FAU (X and Y) frameworks have been thus obtained, *i.e.*, either due to one/two carbonate species formed in NaX from CO_2 and H_2O or due to the extraction of one Al atom during the HY dealumination with the next formation of the hydrated $AlOH(H_2O)_2^{+2}$ species. These deformations of the HY framework lead to the YM variation of HY structure of -7.0 % (without final Al/Si replacement at the empty T position) being comparable with the influence of -5.2 and -5.7 % for one and two carbonate species per UC of NaX, respectively, at the same PBE/PAW level. We would emphasize that we have obtained valuable YM variations upon: 1) relatively soft modification of the system, *i.e.*, the formation of one carbonate / hydrocarbonate species per UC or the extraction of one Al atom per UC; 2) acting on the different parts of the system, either on the framework (HY), or on the cations (NaX).

ACKNOWLEDGEMENTS

The authors thank the financial support of RFFI within the grant 12-03-00749a. The authors acknowledge the Consortium des Equipements de Calcul Intensif (C.E.C.I, supported by the F.R.S.-FNRS, Belgium) and the Plateforme Technologique de Calcul Intensif (P.T.C.I,

supported by the F.R.S.-FNRS, Belgium) for computing resources and Supercomputing Center of Lomonosov Moscow State University for computational time [43].

7. Supplementary Electronic Materials

Supplementary Electronic Materials contain additional Figure S1 being the analogue of Figure 2 for the FF calculations of the energy function *versus* bond Me…O elongations, Figure S2 for the illustration of the "neutralization" of the carbonate charge, the displacements of the MeII cations, Me = Na, K, from their O_i neighbors at the SII (in the 6R) sites of all the systems studied with one (Table S1), and two (Table S2) carbonate species per UC, the bulk and shear modulus upon the carbonate formation (Table S3). Figure S3 illustrates the asymmetry of YM in Cartesian coordinates (in Table S10 in more detail), while the Tables S8-S9 contain the data for Fig. 1 of the main text. The Tables S5-S7 are devoted to the charge analysis.

REFERENCES

[1] P. A. Rebinder and N. I. Likhtman, *Dokl. Akad. Nauck. S.S.S.R.,* 1947, **56**, 7; *Proc. 2nd Intern. Congr. of Surf. Activity (Butterworths)*, 1957, **3**, 295.

[2] A. R. C. Westwood, *Philos. Mag.*, 1962, **7**, 633–649.

[3] J. Hafner, *J. Comput. Chem.*, 2008, **29**, 2044–2078.

[4] W. F. Perger, J. Criswell, B. Civalleri, and R. Dovesi, *Comput. Phys. Commun.*, 2009, **180**, 1753–1759.

[5] (a) G. Kresse and J. Hafner, *Phys. Rev. B*, 1993, **47**, 558–561; b) G. Kresse and J. Furthmüller, *Phys. Rev. B*, 1996, **54**, 11169–11186.

[6] (a) 1. R. Dovesi, R. Orlando, B. Civalleri, C. Roetti, V. R. Saunders, and C. M. Zicovich-Wilson, *Zeitschrift für Krist.*, 2005, **220**, 571–573. (b) R. Dovesi, V.R. Saunders, C. Roetti, R. Orlando, C. M. Zicovich-Wilson, F. Pascale, B. Civalleri1, K. Doll, N.M. Harrison, I.J. Bush, Ph. D'Arco, M. Llunell, CRYSTAL09, User's Manual, 2010.

[7] A. U. Ortiz, A. Boutin, A. H. Fuchs, and F.-X. Coudert, *Phys. Rev. Lett.*, 2012, **109**, 195502.

[8] A.U. Ortiz,. A. Boutin, A.H. Fuchs, and F.-X. Coudert, J. Chem. Phys. 138, 174703 (2013)

[9] F.-X. Coudert, Phys. Chem. Chem. Phys., 2013, 15, 16012–16018

[10] A. Marmier, Z. a. D. Lethbridge, R. I. Walton, C. W. Smith, S. C. Parker, and K. E. Evans, *Comput. Phys. Commun.*, 2010, **181**, 2102–2115.

[11] Wolfram Research, Inc., *Mathematica*, Version 9.0, Champaign, IL, 2012.

[12] P. Ravikovitch, A. Vishnyakov, and A. Neimark, *Phys. Rev. E*, 2001, **64**, 011602/1-19.

[13] P. I. Ravikovitch and A. V. Neimark, *Langmuir*, 2006, **22**, 10864–8.

[14] A. A. Fomkin and A. L. Pulin, *Russ. Chem. Bull.*, 1999, **48**, 1864–1866.

[15] A. V. Neimark, F.-X. Coudert, A. Boutin, and A. H. Fuchs, *J. Phys. Chem. Lett.*, 2010, **1**, 445–449.

[16] A. L. Pulin, A. A. Fomkin, V. A. Sinitsyn, and A. A. Pribylov, *Russ. Chem. Bull.*, 2001, **50**, 60–62.

[17] T. Baimpos, I. G. Giannakopoulos, V. Nikolakis, and D. Kouzoudis, *Chem. Mater.*, 2008, **20**, 1470–1475.

[18] M. Palomino, A. Corma, J. L. Jordá, F. Rey, and S. Valencia, *Chem. Commun. (Camb).*, 2012, **48**, 215–7.

[19] I. A. Bryukhanov, A. A. Rybakov, V. L. Kovalev, and A. V. Larin, *Microporous Mesoporous Mater.*, 2014, **195**, 276–283.

[20] D. M. Ceperley and B. J. Alder, *Phys. Rev. Lett.*, 1980, **45**, 566–569.

[21] J. P. Perdew, K. Burke, and M. Ernzerhof, *Phys. Rev. Lett.*, 1996, **77**, 3865–3868.

[22] M. Hunger, *Solid State Nucl. Magn. Reson.*, 1996, **6**, 1–29.

[23] B. H. Wouters, T.-H. Chen, and P. J. Grobet, *J. Am. Chem. Soc.*, 1998, **120**, 11419–11425.

[24] Z. Yu, A. Zheng, Q. Wang, L. Chen, J. Xu, J.-P. Amoureux, and F. Deng, *Angew. Chem. Int. Ed. Engl.*, 2010, **49**, 8657–61.

[25] G. Kresse and J. Joubert, *Phys. Rev. B*, 1999, **59**, 1758–1775.

[26] R. Hill, Proc. Phys. Soc. A 65 (1952) 349-354.

[27] J. W. Ward, *J. Catal.*, 1967, **9**, 225–236.

[28] J. Datka and B. Gil, *J. Catal.*, 1994, **145**, 372–376.

[29] S. Grimme, *J. Comput. Chem.*, 2006, **27**, 1787–99.

[30] L. Bertsch and H. W. Habgood, *J. Phys. Chem.*, 1963, **67**, 1621–1628.

[31] P. A. Jacobs, F. H. van Cauwelaert, and E. F. Vansant, *J. Chem. Soc. Faraday Trans. 1 Phys. Chem. Condens. Phases*, 1973, **69**, 2130–2139.

[32] A. V. Larin, I. A. Bryukhanov, A. A. Rybakov, V. L. Kovalev, and D. P. Vercauteren, *Microporous Mesoporous Mater.*, 2013, **173**, 15–21.

[33] A. V. Larin, *Microporous Mesoporous Mater.*, 2014, **200**, 35–45.

[34] A. Mace, N. Hedin, and A. Laaksonen, *J. Phys. Chem. C*, 2013, **117**, 24259–24267.

[35] A. Mace, K. Laasonen, and A. Laaksonen, *Phys. Chem. Chem. Phys.*, 2014, **16**, 166–72.

[36] J. J. Pluth, J. V. Smith, J. M. Bennett, and J. P. Cohen, *Acta Crystallogr. Sect. C Cryst. Struct. Commun.*, 1984, **40**, 2008–2011.

[37] A. V. Larin, F. Porcher, E. Aubert, M. Souhassou, and D. P. Vercauteren, *Recent Advances in the Science and Technology of Zeolites and Related Materials Part B, Proceedings of the 14th International Zeolite Conference*, Elsevier, 2004, vol. 154.

[38] I.I. Boldog, A.M. Golub, and A.M. Kalininichenko, *Russ. J. Inorg. Chem.* 1976, **21**, 368-372.

[39] R. D. Shannon, *Acta Crystallogr. Sect. A*, 1976, **32**, 751–767.

[40] A. V. Larin, D. P. Vercauteren, C. Lamberti, S. Bordiga, and A. Zecchina, *Phys. Chem. Chem. Phys.*, 2002, **4**, 2424–2433.

[41] P. Bodart, J. B. Nagy, G. Debras, Z. Cabelica, and P. A. Jacobsf, *J. Phys. Chem.*, 1986, **90**, 5183–5190.

[42] A. G. Pelmenschikov, E. A. Paukshtis, M. O. Edisherashvili, and G. M. Zhidomirov, *J. Phys. Chem.*, 1992, **96**, 7051–7055.

[43] V. Sadovnichy, A. Tikhonravov, Vl. Voevodin, and V. Opanasenko, in *Contemporary High Performance Computing: From Petascale toward Exascale,* ed. J. S. Vetter, CRC Press, Boca Raton, USA, 2013, pp.283-307.

Table 1. BS (cm^{-1}) values for different NaX and NaKX models containing two carbonate and hydrocarbonate species per UC, relative energies ΔU (eV) calculated with LDA or PBE approaches.

Form	Cations	Method	ΔU	BS	
				CO_3^{-2}	HCO_3^-
NaX	153,149	LDA	0.305	73.6	295.8
		PBE	0.000	58.6, 59.7[a)]	332.7, 325.9[a)]
	155,151	LDA	0.000	54.7	433.4
		PBE	0.347	55.0, 67.5[a)]	385.9, 377.9[a)]
	Exper. [30, 31]			60	350
NaKX[a)]	156,152	PBE	0.000	47.3, 68.1, 54.4[a,b)], 59.2[b)]	387.4[a,b)], 386.3[b)]
	153,149	PBE	0.540 0.852[a)] 1.118[a,b)]	128.9, 127.7[a)]	416.8, 414.8[a)]
	155,151		0.448, 1.176[a)] 1.133[a,b)]	91.6, 95.6[a)]	420.0, 407.2[a)]
	Exper. [30, 31]			-	290, 350

[a)] DFT-D2; [b)] Initial introduction of the HCO_3^-/CO_3^{-2} pair instead of two CO_3^{-2} moieties

Table 2. The Cartesian components (E_i), $i = x, y, z$, of the Young's *modulus* (E), bulk (B), shear (S) (all in GPa) modulus according to Hill's form and their variations (in brackets, all in %), UC volume (V, $Å^3$) and its variations (ΔV, %) after Al extraction from 4R fragment as $AlOH^{+2}$ of HY(D) form with different number of water molecules relative to the moduli of HY form calculated at the PBE/PAW level.

Type	N (H_2O)	E_x	E_y	E_z	E	B	S	V (ΔV)
HY	0	39.65 (0.0)	43.04 (0.0)	39.05 (0.0)	39.83 (0.0)	34.56 (0.0)	15.22 (0.0)	3878.3 (0.0)
HY(D)	2	38.67 (-2.5)	35.75 (-16.9)	36.63 (-6.2)	35.89 (-9.9)	26.23 (-24.1)	14.11 (-7.3)	3868.7 (0.24)
	3	38.15 (-3.8)	38.65 (-10.2)	36.18 (-7.3)	36.95 (-7.2)	28.83 (-16.6)	14.36 (-5.7)	3878.4 (2.6×10^{-3})
	4	37.84 (-4.6)	39.82 (-7.5)	35.02 (-10.3)	37.03 (-7.0)	29.30 (-15.2)	14.36 (-5.7)	3877.7 (-1.5×10^{-2})

Figure captions

Figure 1. (a) Cell volume variation ΔV (%) and (b) Young's *modulus* (according to Hill's form) variation ΔE (%) calculated at the DFT level using LDA and GGA PBE methods in the NaX or NaKX zeolites (the color version is on-line). The data for each 4 models with one and two carbonate species per UC are on the left and right, respectively; see them in Tables S8 (a) and S9 (b) in the increasing energy order.

Figure 2. The geometries of carbonates (a, c, d) and hydrocarbonates (b) in the NaX (a, b) and NaKX (c, d) models (the most stable cases from Table 2) optimized using GGA PBE functionals. The M…O_c distances, M = Na, K, are in Table S7. The color assignment corresponds to that in the Figure 2, cyan and blue colors are for K and Na, respectively.

Figure 3. Energy variation ΔU per UC (eV) calculated at the DFT level using LDA (circles) and GGA PBE (triangles, diamonds) methods *versus* a sum of displacements of the Me cations from their O_i neighbors at the 6R sites (SII) *versus* $\Sigma_{i=1,\,M}\Delta R_{Me\text{-}Oi}$ (Å) upon the influence of (a) one (M = 3) and (b) two (M = 6) carbonate (or hydrocarbonate) species per UC relative to in the NaX, Me = Na (circles, triangles), or NaKX, Me = K (diamonds), zeolites without carbonates. The systems with one hydrocarbonate species are shown by circles in (b).

Figure 4. The geometries of the HY (a) and HY(D) forms (b-d) after the $AlOH^{+2}$ formation with 2(b) , 3(c), 4(d) water molecules all optimized at the PBE/PAW level. The atomic colors are given in red, yellow, magenta, and grey for O, Si, Al, and H, respectively.

Figure 5. The O-H frequencies (cm^{-1}) *versus* |O-H| bond length (Å) in the HY framework optimized at the PBE/PAW level (circles). Experimental IR data are given by dot-dashed (ref. [28]) and dotted (ref. [27]) lines. The fitted linear approximation for calculated O-H frequencies is shown by dashed line (correlation r = -0.998).

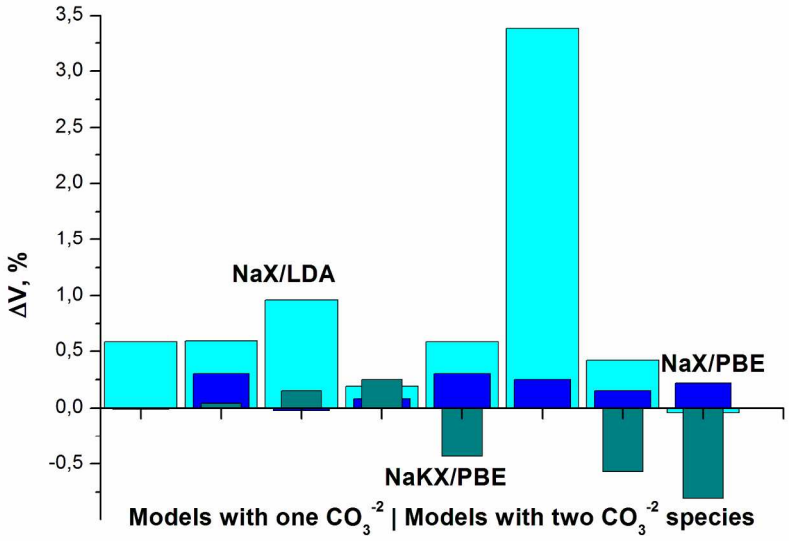

Figure 1a
382x268mm (150 x 150 DPI)

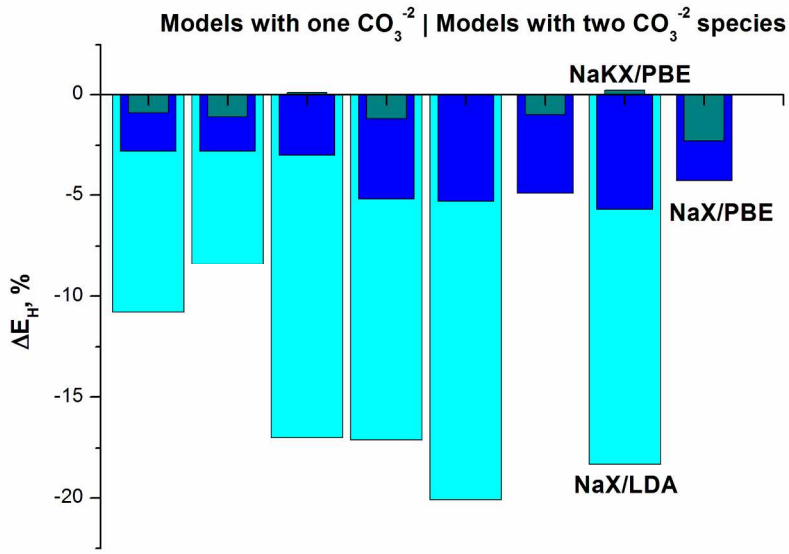

Figure 1b
382x268mm (150 x 150 DPI)

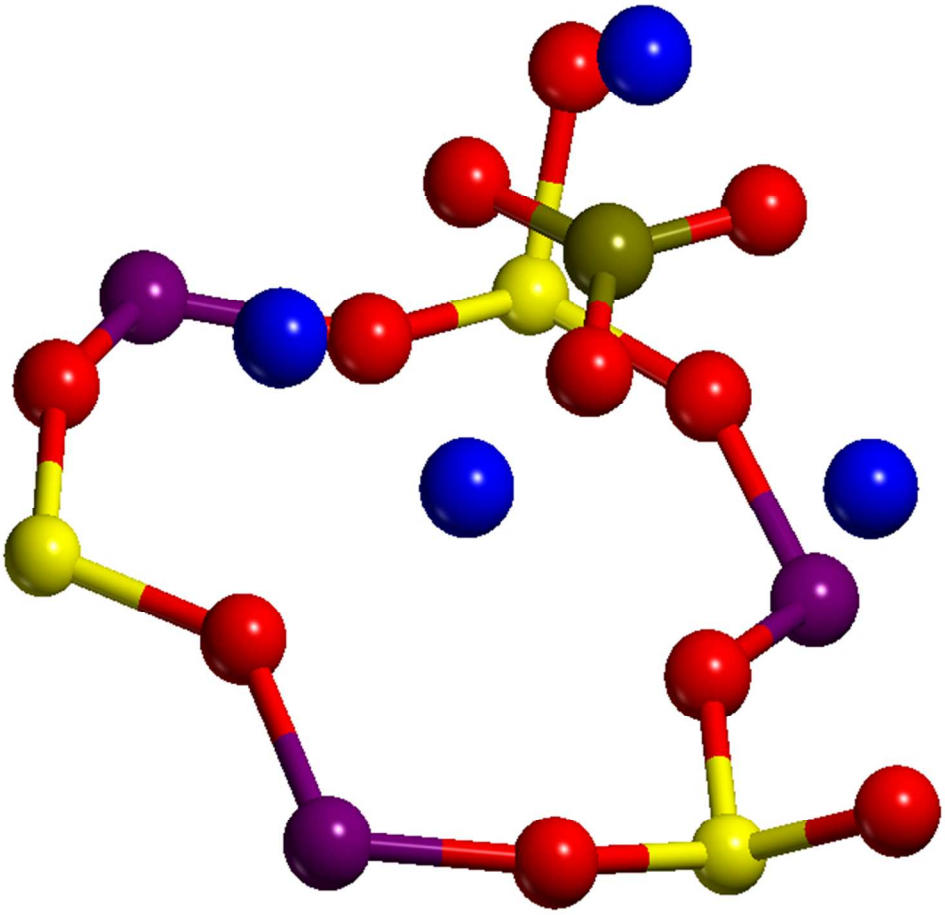

Fig2a
58x54mm (300 x 300 DPI)

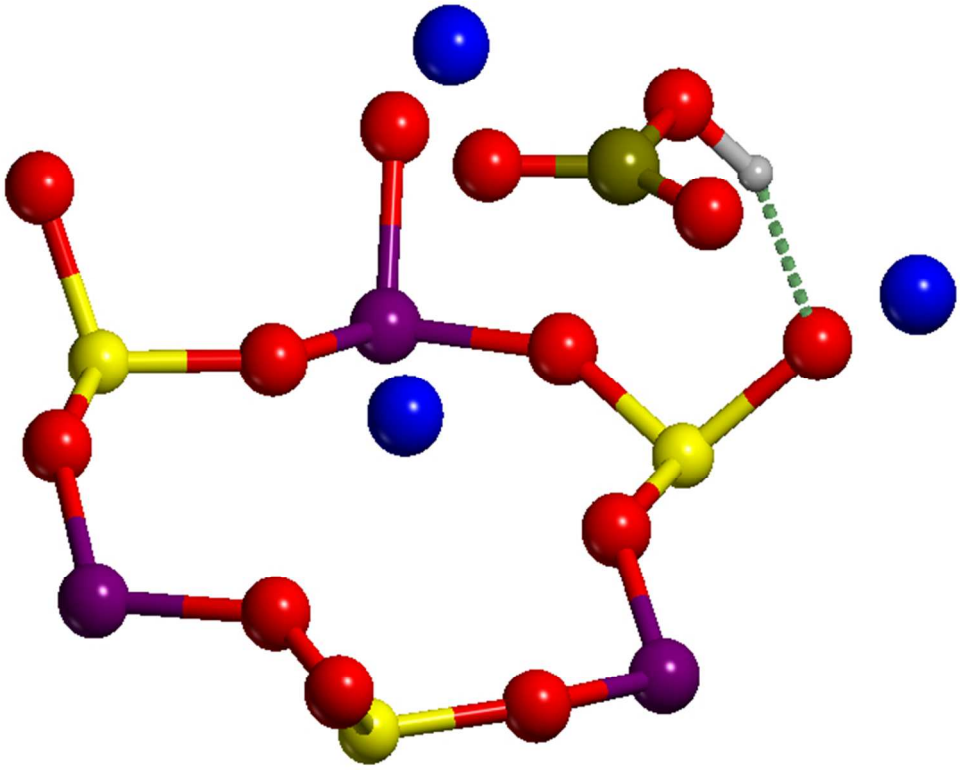

Fig2b
57x45mm (300 x 300 DPI)

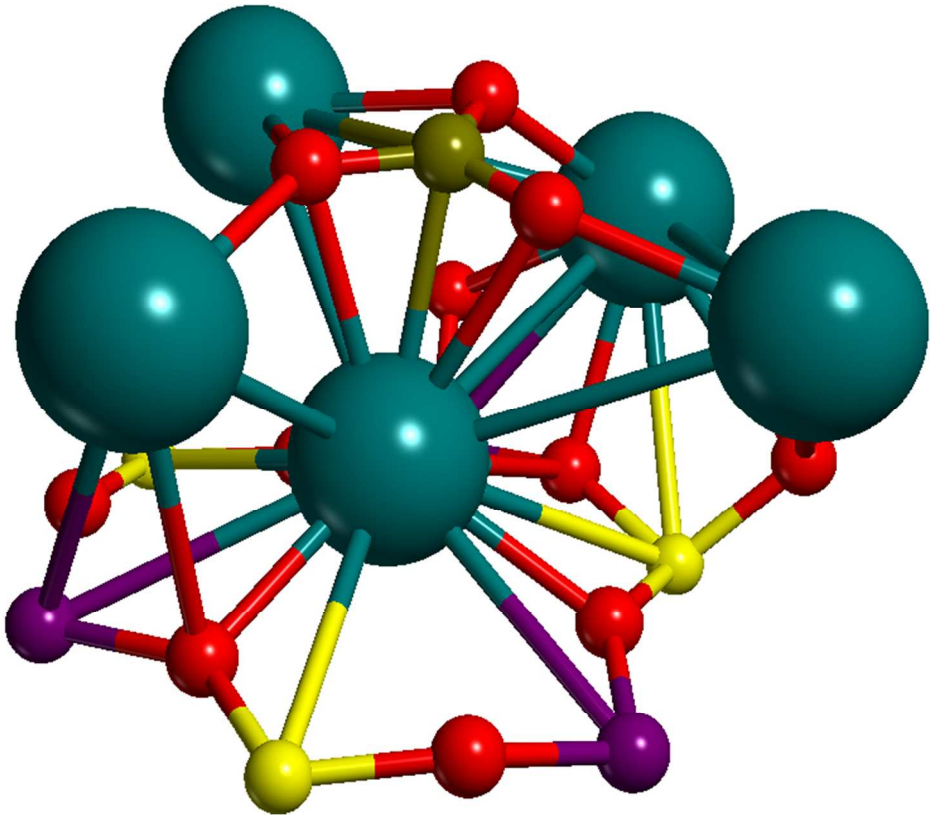

Fig2c
67x54mm (300 x 300 DPI)

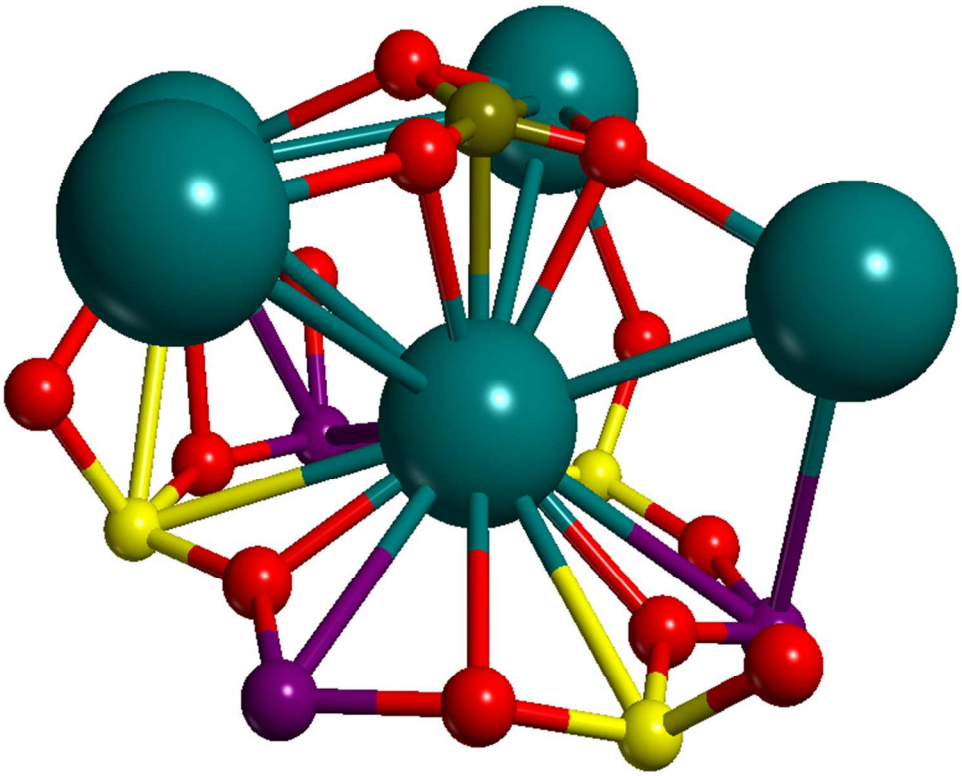

Fig2d
68x53mm (300 x 300 DPI)

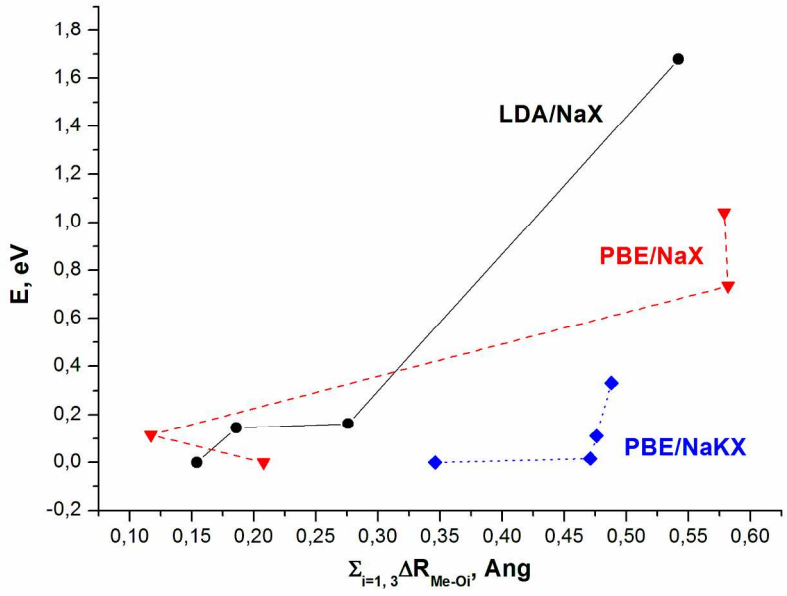

Fig3a
382x268mm (150 x 150 DPI)

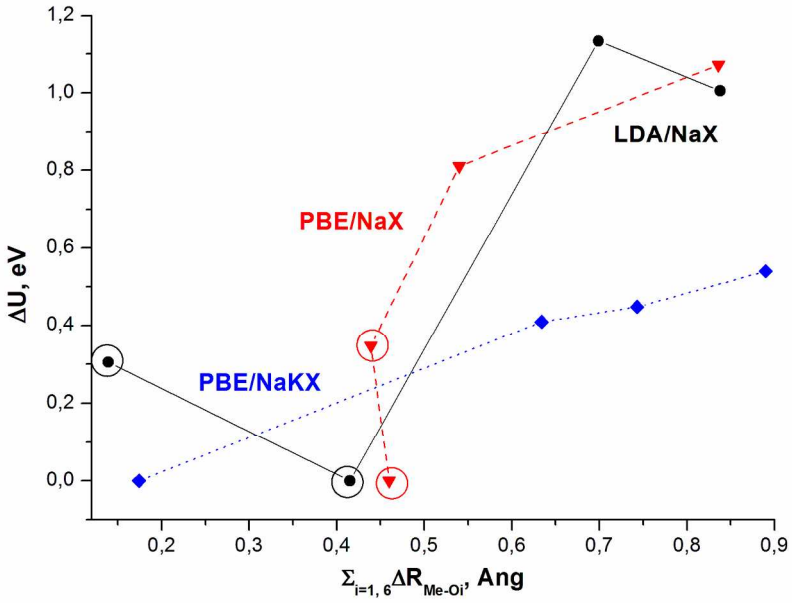

Fig3b
382x268mm (150 x 150 DPI)

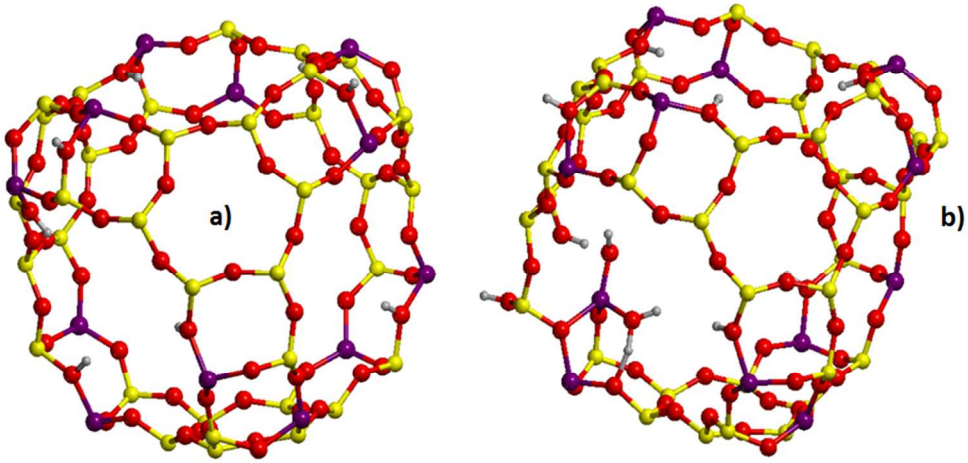

Fig4ab
84x42mm (300 x 300 DPI)

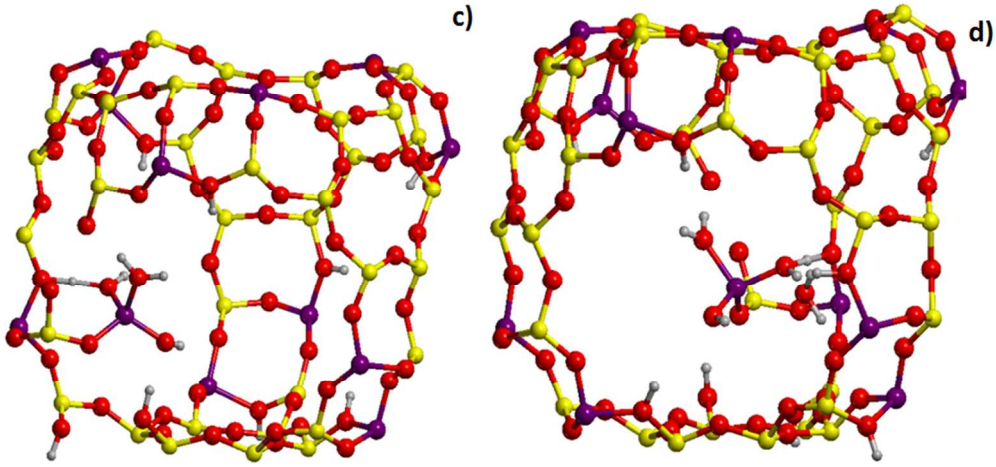

Fig4cd
82x39mm (300 x 300 DPI)

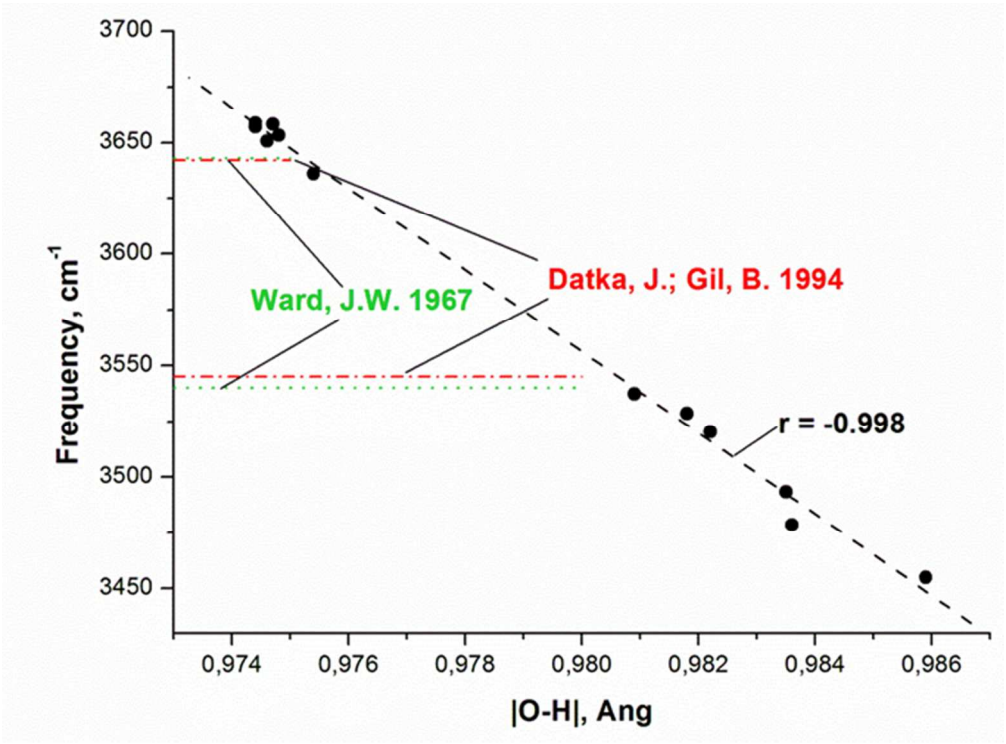

Fig5
57x42mm (300 x 300 DPI)

Figure. The YM values (along OX) averaged *via* Cartesian components *versus* those obtained through standard Hill formulae (along OY) [38] for NaX (circles, triangles) and NaKX (rhombs) zeolites using PBE (rhombs, triangles) and LDA (circles) functionals (according to the data from Tables 2, S9). Correlation 0.979 corresponds to the fit over all the data (solid line) and 0.982 is for NaX only (dashed line).

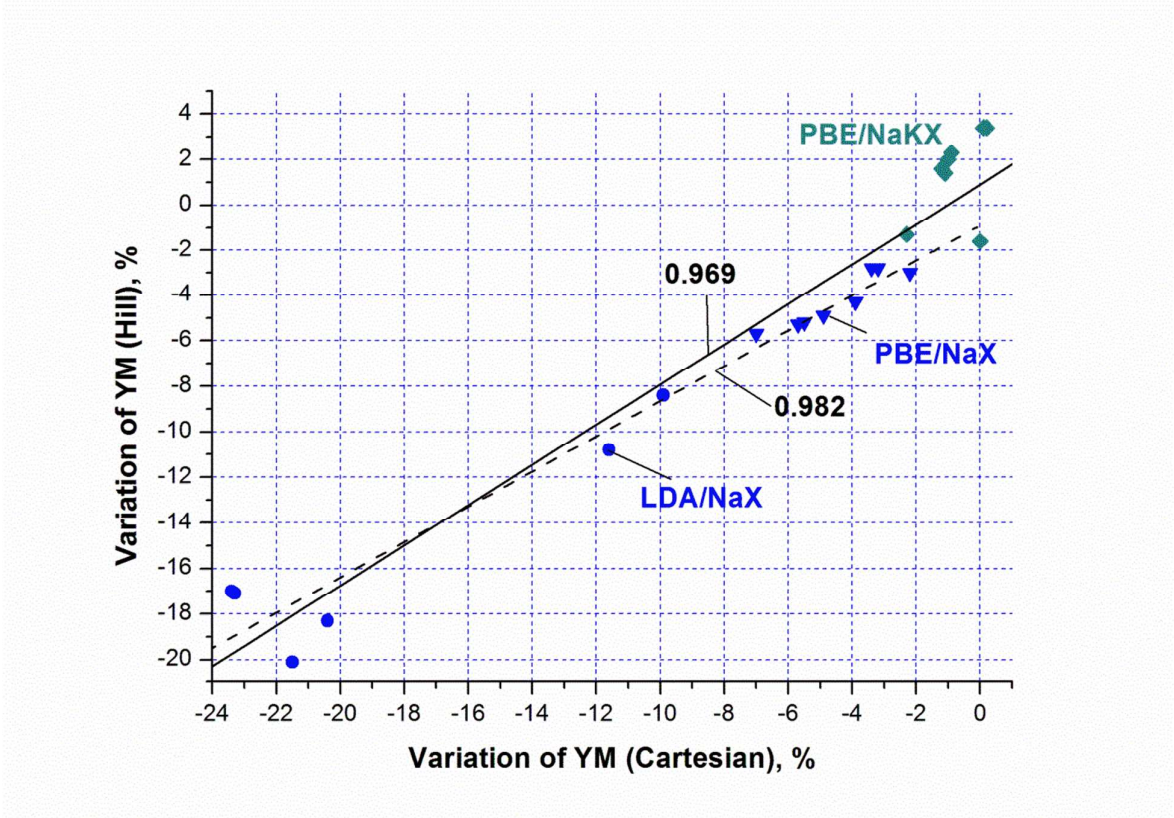

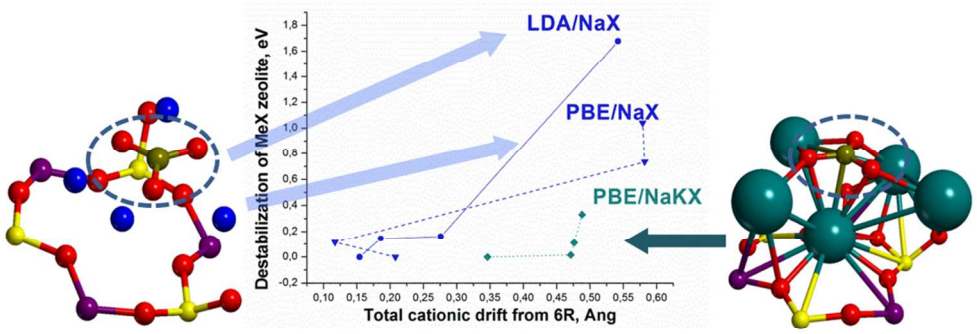

The poorer shielding of CO_3^{-2} species (in ellipses) by Na^+ cations (left) than by K^+ cations (right) results in the stronger NaX destabilization than that of NaKX zeolite at comparable cationic drifts

95x42mm (300 x 300 DPI)